Hybridization of Rubber Tired Gantry (RTG) Cranes

M. Antonelli, M. Ceraolo, U. Desideri, G. Lutzemberger, L. Sani

Department of Energy, Systems, Territory and Constructions Engineering, University of Pisa,
Largo Lucio Lazzarino n. 1, 56122, Pisa, Italy

*Corresponding author: tel. +050 2217311,
email: lutzemberger@dsea.unipi.it

Abstract

Since there is a growing interest worldwide in reducing pollution from sea transport and sea ports activities, one of the biggest issues is to reduce energy consumption and emissions from ground transportation within ports to cranes and other logistic activities. In particular, Rubber Tired Gantry cranes with Diesel engine coupled with electric drive normally brakes the lowering of the container electrically, by dissipating the electric power in resistive loads. This means that energy is consumed to lift the containers and dissipated when it could be recovered, when lowering the load. Thus, one possibility is to recover that energy in a storage system, based on supercapacitors or lithium batteries. This paper starts from experimental measurements conduced on a RTG crane operating in an Italian port. After evaluating real power and energy flows, an appropriate powertrain architecture based on the utilisation of such storage systems was selected, and components properly sized to increase the overall system efficiency. To analyse the different variants and optimize the energy management strategy, a simulation model realised in Modelica language has been used, in order to investigate the cost-effectiveness of the different proposed solutions.

Keywords: hybrid propulsion system, lithium battery, Modelica, rubber tired gantry, supercapacitor

List of acronyms

AUX: Auxiliary loads

BSFC: Brake Specific Fuel Consumption

ED: Electric Drive

EG: Electricity Generator

EM: Electric machine

EPC: Electronic Power Conditioner

ICE: Internal Combustion Engine

PC: Primary Converter

PMM: Power Management Module

RESS: Rechargeable Energy Storage System

SOC: State of Charge

1. Introduction

There is a growing interest worldwide in reducing pollution from sea transport and sea ports activities. The International Maritime Organization (IMO) has adopted MARPOL (International Convention for the Prevention of Pollution from Ships) in 1973. Since then six annexes have been included, that latest of which sets the limits to sulphur and nitrogen oxides emissions from ships. The EU and the USA as well as other areas in the world, from seaports to the waters within 200 nautical miles from the coast, have enforced the strictest limits of 0.1% sulphur content in emissions of ships since 2015. Northern Europe has also enforced the limits of NO_x emissions for new vessels since 2016.

Together with the regulations concerning vessels, ports are organizing themselves in order to be cleaner and smarter. One of the biggest issues is cold ironing that could stop polluting emissions of ships when they are on shore at harbors. The other issues are to reduce and optimize energy consumption and emissions from ground transportation within ports to cranes and other logistic activities (refrigerated containers, storage silos and buildings, access of transportation means from roads and railways).

Diesel engines power most of the moving cranes on sea harbors, since this was the easiest and more flexible way to guarantee mobility and service. Shipside cranes, which have a limited mobility, often on rails, are now being transformed to use electric power. In the best cases, they also feature electricity recovery when lowering the containers, by breaking using the electric motors as generators and exchanging power with the electric grid.

Rubber tyred gantry cranes (RTG), which move containers on the platform to organize storage in piles, after they are unloaded from container vessels, and load them on trucks, are still powered by diesel engines, which are used as electric power generators for motors that lift and lower containers and move the system on the ground.

RTG with Diesel engines coupled with electric drives normally brake the lowering of the container electrically by dissipating the electric power in resistive loads. This means that energy is consumed to lift the containers and dissipated when it could be recovered when lowering the load.

The problem was first mentioned by Kuilboer [1] who described a new concept of RTG drive system developed by Siemens. Three years later a Master of Science thesis at TU Delft [2] was published about the energy management of RTG cranes equipped with a hybrid drive with ultra-capacitors. The calculations of energy and fuel saving were based on the port of Felixstowe in the UK, which had also been mentioned in [1] as a test case for the Siemens concept.

The Equivalent Consumption Minimization Strategy (ECMS) proposed in [2] is used to determine the exact performance set points for the motor and the ultra-capacitors and thus minimize fuel consumption. ECMS was used by Siemens in their ECO-RTG drives for RTG cranes and was further studied by Mulder [3], who predicts saving of over 55 000 USD per year for ten years in excess of the payback of the investment for cranes equipped with that system.

Other studies have been presented [4] [5] [6] about the port of Felixstowe and about the benefits of the hybrid drive approach based on Siemens control strategies, but in all cases there is no real application of the technology but only more accurate and complete simulations of the RTG working cycles, control strategies and economic benefits.

Another approach with some experimental results was followed by Flynn, et al, [7] [8] who studied the use of flywheel in an RTG crane including a downsizing of the internal combustion engine. Fuel saving is expected to reach 35%.

A research group of the Chinese Air Force Radar Academy in Wuhan [9] [10] [11], has studied an RTG Crane with supercapacitors to store energy proposing a DC/DC bidirectional converter and a voltage equalization method. This study is also based on simulations of a concept and no experimental data are provided, either of the crane or the hybrid drive operation.

The absence of real applications is also mentioned by Acciaro and Wilmsmeier [12], who ask for agreed indicators and energy consumption inventories in the maritime and port sector and highlight the lack of awareness of port operators for the energy consumption and efficiency of their operations.

In fact a couple of years earlier Yang and Chang [13] had proposed the electrification of RTG cranes as a measure for reducing energy consumption in ports. The need for sustainable and efficient seaport operation was also called in [14] [15]. None of those papers, even though they were published 10 years later than [1], mentioned the Siemens ECO-RTG as a potential system to reduce energy consumption in RTG cranes.

This means that no real hybrid system seems to be in operation in RTG cranes. This is confirmed by a second Master of Science thesis, again at TU Delft [16], has been published in 2016 with a proposal of a hybrid system using a Lithium-titanate battery. The study is mainly focused on economics and some recommendations are provided concerning the improvement of the simulation of the Diesel engines. The latest contribution in the literature [17] describes the investigation of an electric RTG crane equipped with a battery-supercapacitor system, where the battery replaces the internal combustion engine.

As noticeable, different variants of energy storage systems can be found in literature, such as supercapacitors, lithium batteries or flywheels. Additionally, no experimental data are available from the already mentioned activities on this topic. Indeed, this paper started from the above literature, but the aim is different and the approach is novel.

In fact, the study is based on measurements on an RTG crane operated in the port of Leghorn in Italy. The crane is used to move containers on the shore and to place them on trucks for transportation to the final destination. The crane is powered by an internal combustion engine used as an electrical generator for the rubber tyres and hoist. The engine is oversized to be able to provide the electrical power for the peak power demand, when the container is being lifted. The braking power is also electric, but is dissipated on a resistive load placed on the roof of the electrical control board.

Starting from these experimental measurements, the aim of the activity was to consider the utilisation of energy storage systems to recover at least partially the energy otherwise dissipated. Indeed, a powertrain architecture equipped with such storage systems has been chosen, and an opportune energy management strategy defined, in order to improve the overall system efficiency. Different sizes of smaller internal combustion engines and different storage systems technologies have been also considered, in order to identify pros and cons among the different solutions. In this regard, a simulation model has been created in Modelica language [18], to analyse performance for the examined configurations. Finally, a cost-benefit analysis for the different variants was also presented.

Naturally, the installation of new components on-board the RTG crane implies several layout studies and mechanical analysis, to maintain the same level of safety and stability. The analysis, not presented in this paper, could be performed according to the approach followed in [19] [20].

2. The conventional RTG crane

2.1. The conventional powertrain

The conventional RTG crane is typically employed in shipping ports, to move containers up to around 40 tonnes. Figure 1 shows the conventional powertrain of the RTG crane under analysis.

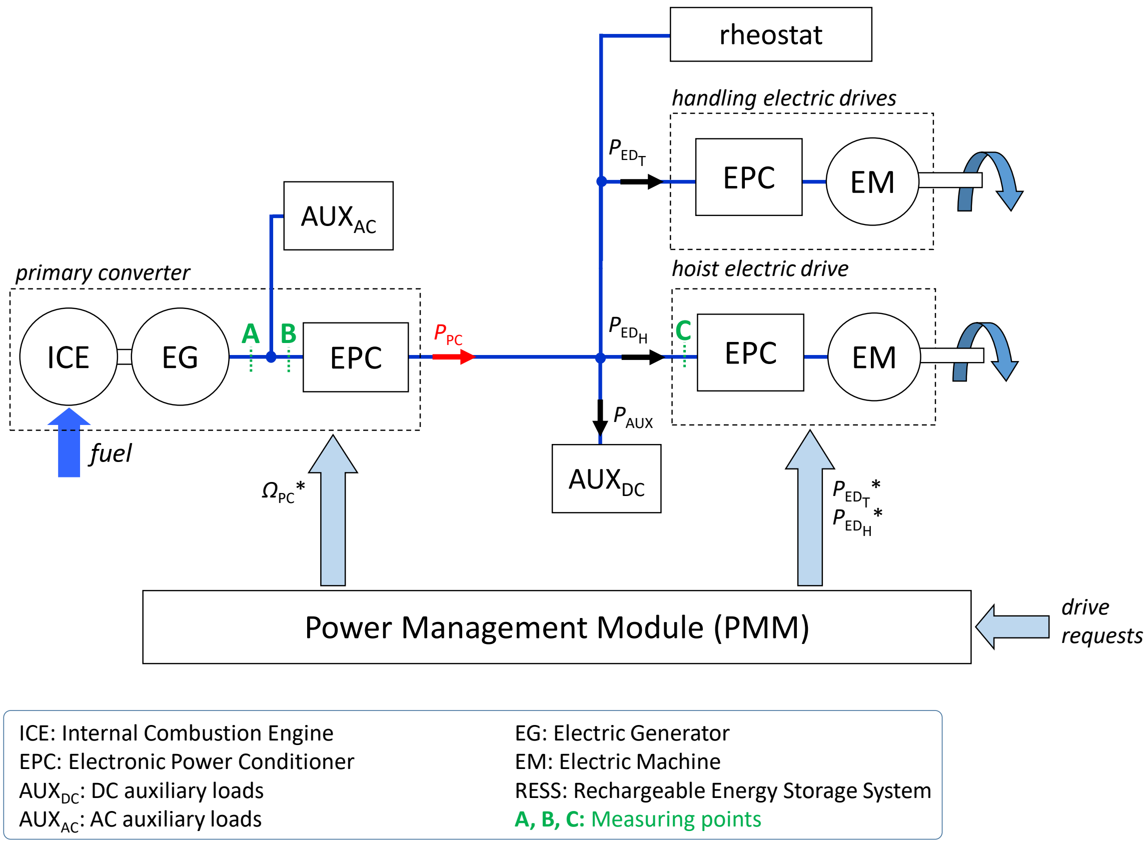

Figure 1. Conventional powertrain for the RTG crane

The conventional powertrain consists of a Diesel engine (ICE) coupled to an electrical generator (EG), which provides electrical power to a set of electric drives, employed in hoist operations, i.e. lifting and lowering of containers, and handling operations, i.e. in the movement of the gantry and of the trolley. In this configuration, the Power Management Module (PMM) simply transfers the operator control requests to the electric drives, typically imposing the ICE speed at a constant value. Indeed, when the container is lifted, the ICE provides the energy demand to the hoist electric drive. On the other hand, when the container is lowered, potential energy is converted into electrical energy. Despite this, due the absence of one storage system, this energy cannot be stored and is wasted on some resistor banks (rheostat). Finally, as visible in Figure 1, several AC and DC auxiliary loads of the RTG crane are present. As visible, AC loads are located to the output port of the electrical generator (EG). Thus, for feeding them at the correct frequency (50 Hz), the primary converter has to rotate at an imposed, fixed speed.

2.2. The experimental tests

Experimental tests were made in collaboration with the shipping port of Livorno, with the aim to analyse energy flows during typical working operations, (i.e. raising or lowering) of the containers. In particular, one RTG crane has been equipped with some data sensors, to acquire the electrical energy flows. The measuring points (A, B, C) were shown in Figure 1, green coloured (A, B, C). The energy flow measured in A represents the electrical energy generated by the alternator, coupled to the ICE. This is the full amount of the electrical energy produced, before the adsorption of the AC auxiliary loads. Then, B represents the energy flow available at AC bus, after the adsorption of the AC auxiliary loads. Finally, it was measured the electrical energy managed by the hoist electric drive, adsorbed when working as motor during lifting operations, produced when working as generator during lowering. In the measurement campaign, several days have been considered: results were shown in Table 1, where the number of ascents and descents was also indicated.

Table 1. Measurements of energy flows in some of the considered days

Date	*31/05*	*03/06*	*07/06*	*13/06*	*17/06*
Energy produced PC (A) (kWh)	139.5	113.9	634	108.7	95.9
Energy produced PC (B) (kWh)	121.2	100.8	54.7	87.2	73.4
Energy hoist ED mot (C) (kWh)	93.0	72.2	38.5	57.0	37.5
Energy hoist ED gen (C) (kWh)	63.1	49.1	24.7	36.4	19.2
$E_{hoist\ gen}/E_{produced}$ (%)	45.2	43.1	38.9	33.5	20.0
Number of ascents	205	143	89	127	79
Number of descents	189	136	84	113	90

As noticeable, the ratio between the recovered energy during lowering operations and the produced energy by the alternator is typically in the range between 34% and 45%. Indeed, if stored, that energy could be re-used during this amount of energy could be reused during the lifting of the container, consequently reducing the energy generated by the alternator coupled to the ICE.

The analysis of energy flows has been used also to identify typical duty cycles during working operation. Lifting and lowering phases have been analysed separately, identifying the power requests, number of working cycles and time durations. Figure 2 shows results of the analysis of the duty cycle regarding lifting.

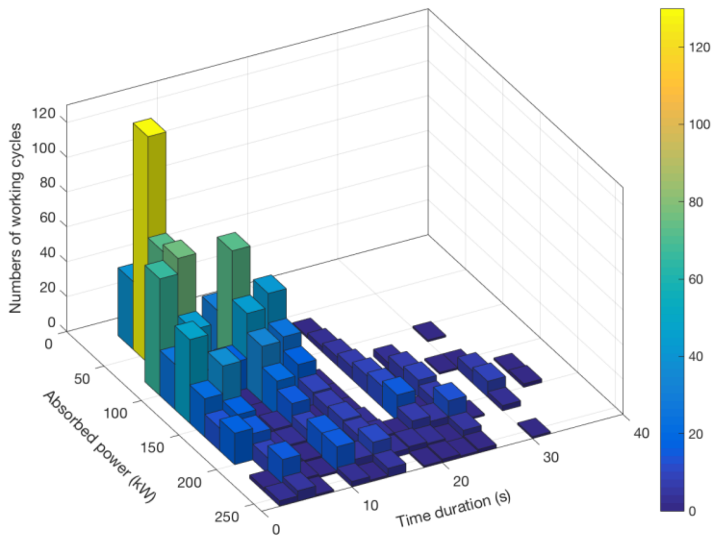

Figure 2. Combined analysis of working cycles, lifting operation

As visible, the main concentration of working cycles in lifting operation is comprised within 250 kW and 15 s. As noticeable, the majority of the considered duty cycles are included in this range. The same approach has been followed in classifying cycles corresponding to lowering operation, shown in Figure 3. In addition, the majority of them is comprised in the same identical previous range, i.e. within 250 kW and 15 s.

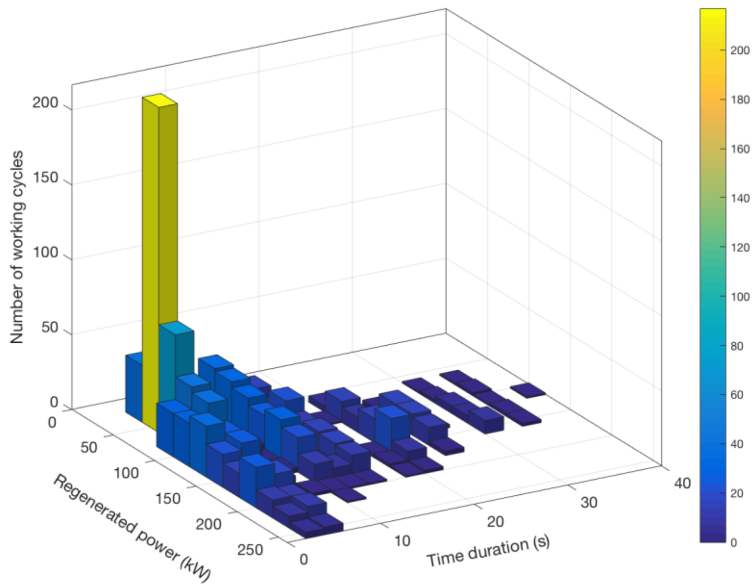

Figure 3. Combined analysis of working cycles, lowering operation

3. Hybrid propulsion system design

The hybridization of the conventional system can be made by simply introducing, directly connected to the DC bus, one storage system. The aim was to recover the energy produced by the hoist electric drive, during lowering phases. The following paragraphs show the preliminary design of the hybrid powertrain architectures, the proposed energy management strategy and the preliminary sizing of components.

3.1. Hybrid powertrain architecture

Since the conventional powertrain is already characterised by the presence of the electrical generator and the DC bus, the easier conversion regards the implementation of a series-hybrid architecture, shown in Figure 4 and taken as reference. As visible, the needed power is firstly converted into electricity, and the sum of energy between the two power sources is made in terms of electric quantities in an electric node. The presence of a Rechargeable Energy Storage System (RESS) allows to recover the electrical energy produced by electric drives, when working as generator, and helps in reducing the size of the primary converter. As noticeable, AC loads have been connected, through the introduction of a DC/AC converter, directly on the DC bus. Although the presence of an additional component might result disadvantageous in terms of costs and volume occupation, feeding of AC loads directly from DC bus allows to control the primary converter at variable speed, giving much more flexibility in the implemented energy management strategy. The energy management strategy is implemented inside the Power Management Module.

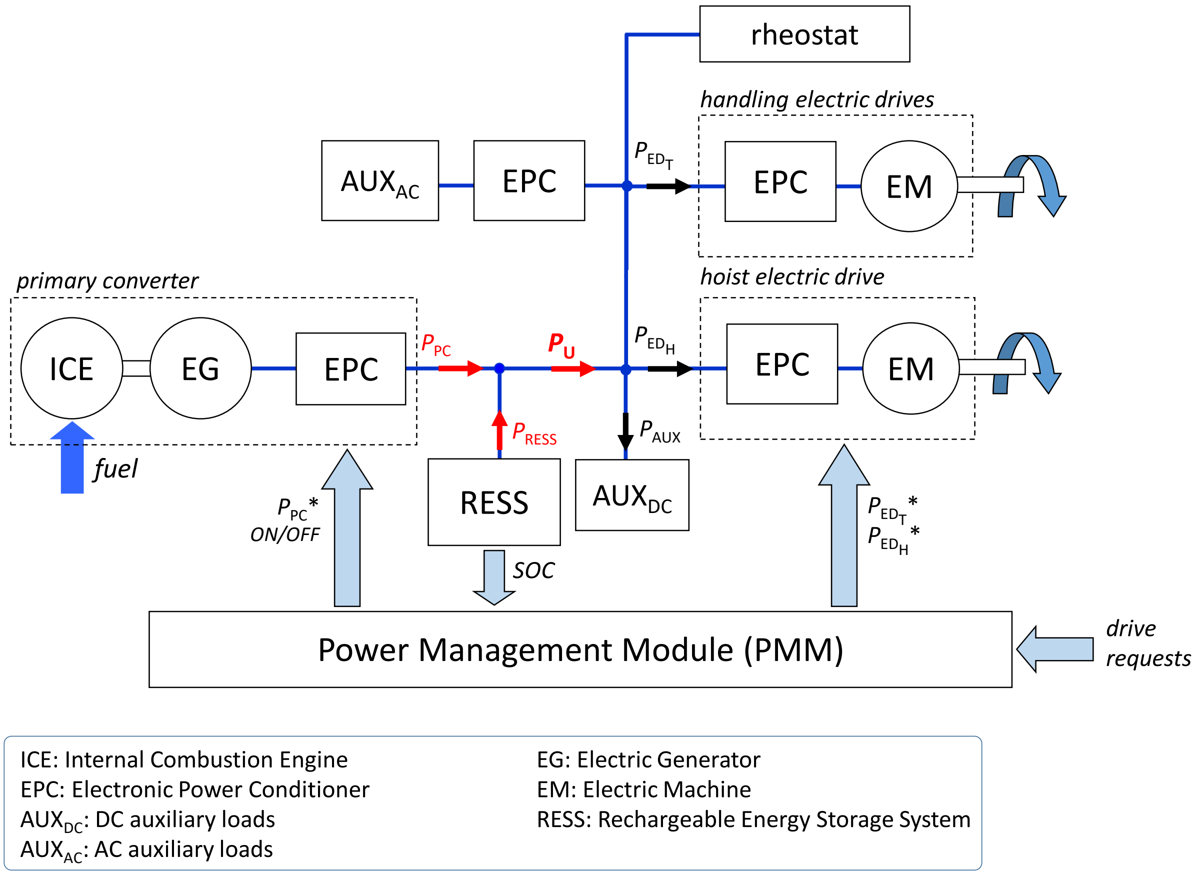

Figure 4. Series hybrid architecture for RTG crane

3.2. Energy management strategy

The Power Management Module determines, as a function of the operator's requests and possible other signals, which part of the requested propulsive power must be delivered by the primary converter (PC) and which by the rechargeable energy storage system (RESS). The purpose of determining the share of the useful power between the two sources has been already described by the authors in some other case studies, with much more details in [21] [22]. Here is just reminded that:

- $P_U(t)$ is determined to answer the operator's commands as closely as possible. It is a direct consequence of the working duty cycles, in which hoist, trolley and gantry operations have to be included.
- $P_{AUX}(t)$ is given by the AC and DC auxiliary loads.
- $P_{PC}(t)$ is determined by PMM according to some optimization rule.
- $P_{RESS}(t)$ is automatically determined by difference.

It must also be noticed that the *useful* power $P_U(t)$ can be imagined to be constituted by an average value and ripple. Indeed, it is possible to control the system such as the ripple $r(t)$ is delivered by the RESS and does not form part of the primary converter. Hence, the primary converter delivers only average powers, working at fixed or slowly variable points. The RESS manages the ripple component $r(t)$ of the needed useful power, with the addition of some additional average power, to avoid SOC deviation during normal operating conditions. The strategy presented above requires also the consideration of the future system load [23].

After determining $P_U(t)$ an internal algorithm is used to choose the optimal values of the ICE rotary velocity, corresponding to the minimum fuel consumption. Additionally, also ON/OFF strategy of the primary converter can be implemented to switch off the ICE when average load powers falls in a poor efficiency region. Further details about implementation of ON/OFF strategy are described in [24].

3.3. The simulation model

The simulation activity has been performed through Modelica language, an open source environment specifically developed for modelling and simulation of complex engineering systems [18].

According to the modelling approach already used in [21] [22], the system shown in Figure 4 has been modelled, and all the subsystems have been represented with the needed accuracy. According to Figure 4, the main subsystems have been here briefly described:

- Primary converter, composed by an internal combustion engine (ICE), an Electrical generator (EG) and the power converter (EPC). The model for the ICE used the BSFC maps, i.e. fuel consumption maps. The model can emulate the engine torque and fuel flow, dependent on throttle position and engine speed. It contains inertia load and a start-up logic, when ON/OFF strategy is considered [25]. Regarding electric components, in many circumstances the dynamics to be considered for this kind of analysis are much slower than the faster electric dynamics. In these cases, the only state variables to be considered can be those related with the mechanical inertias of the rotating parts. The rest can be modelled as being algebraic, i.e. with maps containing operating region and efficiencies [25].

- Rechargeable energy storage system (RESS), composed by electrochemical lithium batteries or supercapacitors. The model has been dealt through an electrical network composed by an electromotive force, an inner resistance and *n* RC blocks. Choice of *n* is determined by a compromise between complexity and precision [26].
- About auxiliary loads (AUXs), handling and hoist electric drives (EDs), they have been not represented inside the model. The corresponding load requests have been directly imposed at the DC node, from the knowledge of the measured electric power profiles.

4. Sizing of subsystems

4.1. Internal Combustion Engine

The sizing of the internal combustion was performed by analysing the working load cycles followed by the gantry, measured during the observation period. As first observation, if the average power delivered by the original ICE is evaluated, we can find that this value is significantly lower than the nominal one. If the total energy delivered by the engine is divided by the overall time, values ranging from 13 kW up to 18 kW (depending on the day) are obtainable. Finally, if the reference time is reduced to the time in which the engine was effectively running, thus neglecting the periods in which the gantry was shut down, higher but still quite low values can be encountered (from 16 kW up to 25 kW).

It is clear that the employment of the hybrid architecture shown in Figure 4 can greatly reduce the sizing of the ICE. For this sake, based on the above mentioned values, different alternative gen-sets (i.e. primary converters) were taken into account, whose installed powers ranged from 28 kW up to 320 kW (case from 1 to 9 in Table 2). The possibility of keeping the original ICE, having 414 kW, was also taken into account (case 10 in Table 2).

Table 2. Maximum power of the analysed diesel gen-sets

<table>
<tr><th rowspan="2">Case n.</th><th rowspan="2">Max power (kW)</th><th colspan="4">BSFC (g/kWh) vs. load</th><th rowspan="2">Rotating speed (rpm)</th></tr>
<tr><th>100%</th><th>75%</th><th>50%</th><th>25%</th></tr>
<tr><td>1</td><td>28</td><td>285</td><td>301</td><td>301</td><td>365</td><td rowspan="10">1800</td></tr>
<tr><td>2</td><td>36</td><td>271</td><td>271</td><td>282</td><td>324</td></tr>
<tr><td>3</td><td>54</td><td>285</td><td>296</td><td>302</td><td>358</td></tr>
<tr><td>4</td><td>69</td><td>267</td><td>267</td><td>282</td><td>338</td></tr>
<tr><td>5</td><td>117</td><td>231</td><td>237</td><td>253</td><td>302</td></tr>
<tr><td>6</td><td>139</td><td>231</td><td>232</td><td>244</td><td>290</td></tr>
<tr><td>7</td><td>165</td><td>244</td><td>268</td><td>269</td><td>308</td></tr>
<tr><td>8</td><td>230</td><td>214</td><td>219</td><td>229</td><td>266</td></tr>
<tr><td>9</td><td>320</td><td>230</td><td>229</td><td>248</td><td>283</td></tr>
<tr><td>10</td><td>414</td><td>196</td><td>202</td><td>215</td><td>256</td></tr>
</table>

For a first assessment of the fuel consumptions, the following hypotheses were assumed:

- The original ICE (i.e. the 414 kW) is used at fixed rotating speed in the conventional powertrain architecture depicted in Figure 3 (see Section 2.1). The fuel consumption was calculated starting from evaluation of the average power required in the measured working load cycles, and using fuel consumption data at different engine loads, as provided by the manufacturer. This was used to calculate a reference fuel consumption, to be compared with those obtained from the hybrid variants.
- The downsized ICEs in the hybrid variants have been used in agreement to the described energy management strategy, i.e. working at fixed or slowly variable power, and rotating speed is chosen to minimize the fuel consumption, also including the presence of ON/OFF strategy. In this regard, a reference BSFC map was then downscaled to be representative for different sizes, with specific fuel consumptions aligned to what shown in Table 2.
- The RESS was modelled as a generic energy storage, having a charging/discharging efficiency at constant value of 0.85.

As noted from Figure 5, the variable load is mainly satisfied by the RESS, while the ICE works at slightly variable power, when it is able to work in its maximum efficiency zones, or it is switched off. When the ICE is switched on after off periods, rising edges of power are determined by the difference between actual and reference SOC. Clearly, this reference value must be selected within a defined window range, to allow energy recovery during the descent of the hoist, and energy release during climb operations.

The choice of the ICE sizing clearly affects the engine cycle load shape, as always shown in Figure 5, top and bottom (with the 47 and 165 kW diesel gen-sets, respectively). A smaller size implies, according to the energy management strategy implemented, one substantially constant utilization of the ICE itself, and one deeper discharge of the RESS, as shown in Figure 6. Regenerative braking during the lowering of the load has been considered in all the presented case studies.

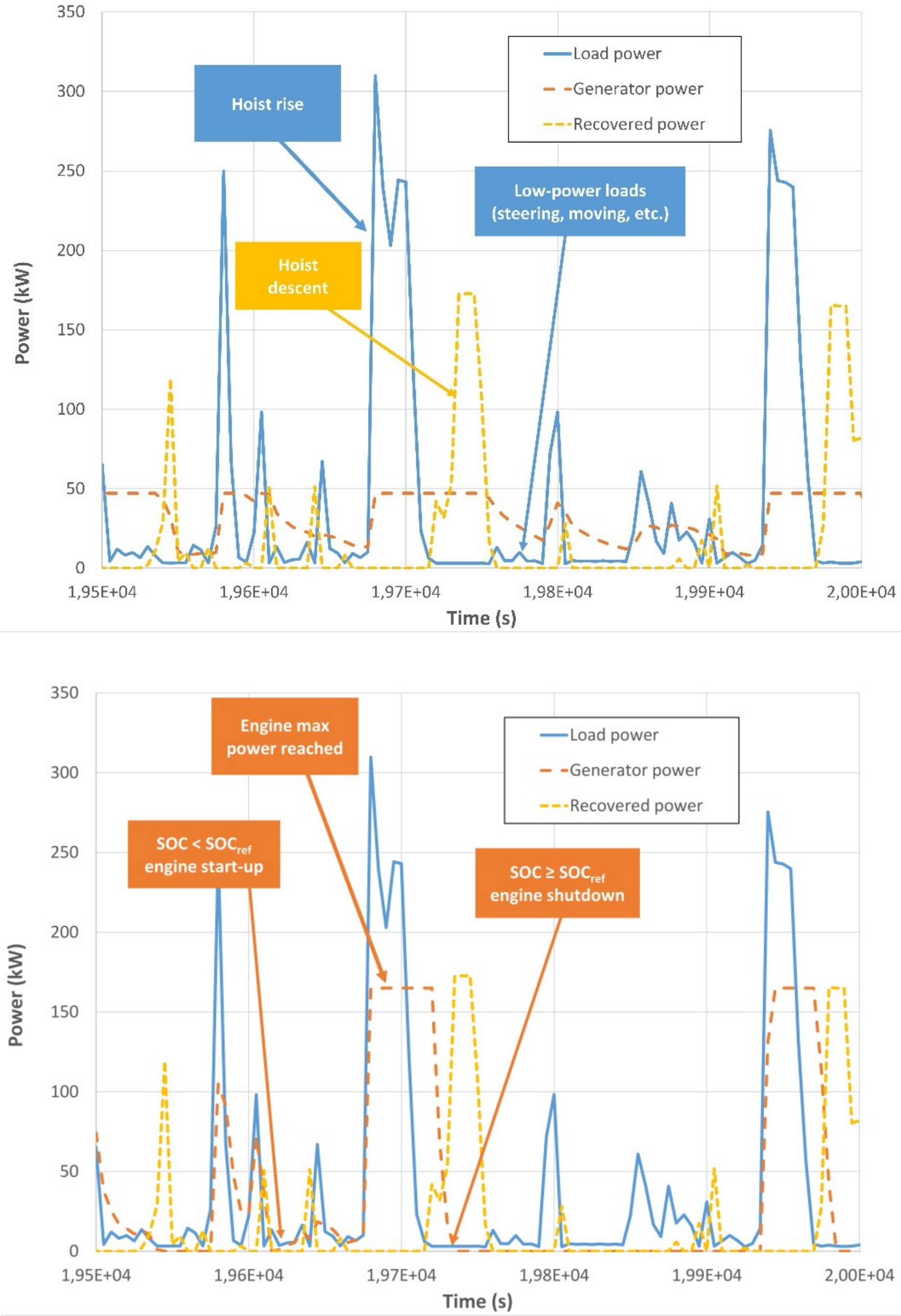

Figure 5. Load cycle with 47 kW (top), 165 kW (bottom)

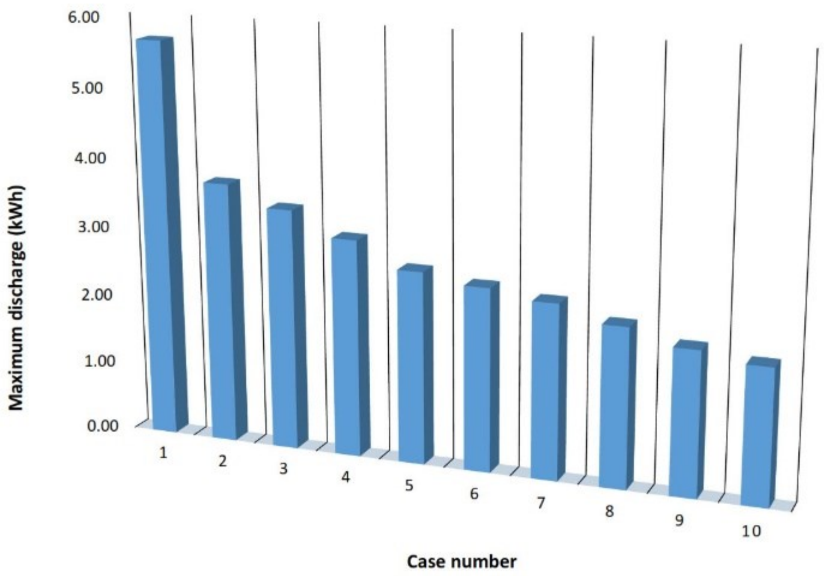

Figure 6. RESS maximum discharge with descending loads regeneration (right)

The choice of the diesel gen-set also had a noticeable influence on the fuel consumption; the trend however (Figure 7) shows a clear dependency between the size of engine and the consumption. In effects, smaller engines are operated for much time at their design point, but larger engines had better BSFC performance in absolute. The trend was not strictly monotonous since the result depended upon the fuel economy features of each engine. Results shown in Figure 7, apart downsizing of the ICE with the considered energy management strategy, include the descending loads regeneration. It must additionally be stated that regeneration influences by itself of about 20% the fuel saving percentages shown in Figure 7.

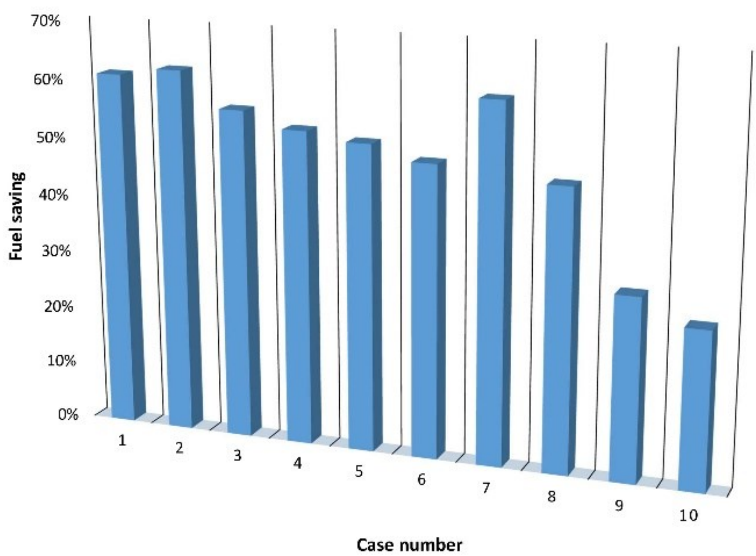

Figure 7. Fuel saving including descending loads regeneration (right)

The possibility of recovering the energy during the descents of the hoist naturally has a great influence on the sizing of the RESS and of the ICE. As example, energy recovery capability allows a significant contribution in RESS re-charging during descend operations. Thus, RESS is quickly brought back at the reference SOC also in case of a small ICE, thus guaranteeing to avoid SOC drifts. If SOC drifts occur, a larger RESS must be considered, having the ICE not enough power to quickly recharge the RESS before the subsequent ascent of the load. However, hybrid architecture necessarily implies the presence of electric drives capable of energy recovery, as will be anyhow assumed in the RESS sizing, as shown in next paragraph.

As a summary, this first analysis highlighted that the recovery of the descending loads and the reduction of the diesel engine size, also with the considered energy management strategy, provides a noticeable fuel saving, about 60% respect to the original configuration. However, the fuel saving increase is smaller and smaller below a certain engine size. As visible, utilisation of the original ICE in a hybrid architecture is still able to guarantee a significant fuel reduction, around 30%.

4.2. Storage system

At preliminary stage of analysis, three different variants of storage systems have been considered:

- System based with energy oriented lithium cells.
- System based with power oriented lithium cells.
- System based with supercapacitors.

For every typology, one reference cell has been selected from available market products. The, storage system has been sized, to form the battery pack or the supercapacitor stack. According to the working cycles shown in Figure 2 and Figure 3, two main stress conditions were taken into account. The first one is related to the most frequent maximum power, required or adsorbed, identified in 250 kW. The second one refers to the most frequent maximum energy, to be delivered or stored, when 150 kW for 15 s are required. When power and energy requests are over the considered range, following assumptions have been made: when power (or energy) is requested, the ICE provides the extra needs. When power (or energy) is generated, rheostat dissipates the extra-need that cannot be stored in the storage system.

4.2.1. Systems based on lithium batteries

This case is related to the installation of one storage system based on lithium cells. Table 3 shows the two considered cells. The first one, based on LFP technology, is energy-oriented and much cheaper than the other one. The cost of the NMC power-oriented cell is justified by the higher performance offered, as visible from the values of specific energy, energy density and specific power shown in the last rows of Table 3.

Table 3. Main characteristics of the lithium cells

	Winston Battery WB-LYP160AHA	**Kokam SLPB80460330H**
Typology	LFP	NMC
Capacity (Ah)	160	100
Voltage max/nom/min (V)	3.7/3.3/2.8	4.2/3.7/2.7
Max discharging current peak (A)	480	800
Mass (kg)	5.6	2.4
Volume (L)	3.8	1.2
Cost (€/kWh)	400	800
Nominal energy (Wh)	520	370
Specific energy (Wh/kg)	93	154
Energy density (Wh/L)	137	308
Specific power (W/kg)	279	771

As visible, maximum peak of discharging current (i.e. under stress conditions of very short time) has been indicated by the manufacturer. On the other hand, maximum peak charging currents are typically not reported, since manufacturers typically considered continuous charging conditions. Indeed, these limits have been assumed symmetric, thus considering the same limits indicated for charging.

The sizing of the battery pack has been performed by evaluating, in reference to the stress conditions already presented, if the selected storage system was able to cover the power/energy requests, under the boundary condition of the DC nominal bus voltage, to correctly guarantee the 400 V AC required by the electric drives, as in other existing applications [22]. Then, if under the maximum power solicitation, the current stays under the maximum allowed peak. Finally, if the storage was able to provide or to store all the required energy, during the considered working cycle. Following formulas have been used:

$V_m = n_s V_{cm}$	(1)
$E_n = \int v(t)i(t)dt \cong V_m Q_E$	(2)
$P_n = v(t)i(t) \cong V_m \frac{Q_P}{T}$	(3)

Where V_{cm} is the average cell voltage, V_m is the average battery voltage, E_n and P_n are the nominal energy and power respectively, Q_E and Q_P represents the electric charge defined by the energy or power requirements, T is the reference charging or discharging time for the considered solicitation. As said, number of cells in series n_s has been determined having as constraint the DC bus voltage (1). Then, battery capacity is chosen in consideration of the energy (2) or power (3) requirements on the considered solicitation, by selecting the highest number between the calculated Q_E or Q_P.

The sizing has been performed also by taking into account the cell life. In this regard, considering the high number of working cycles per day, many hundreds of thousands of charging-discharging cycles must be considered, in the whole life of the plant. Indeed, from experience made by authors on lithium batteries [27], depth of discharge (DOD) under the considered working cycle should not overcome 1%, to avoid the early replacement of the battery pack. Practically, final battery nominal capacity C_n is selected by taking in consideration this further requirement, respect to what already obtained, as visible from formula (4).

$DOD = \frac{Q_{E,P}}{C_n}$	(4)

Where DOD is the imposed depth of discharge under the considered solicitation (i.e. 1%), Q_E or Q_P is the highest electric charge defined at the previous step, while C_n is the final selected nominal capacity.

Table 4 show the corresponding storage system sizing. As noticeable, maximum current and specific power have been analysed in reference to the maximum solicitation in terms of power. On the other hand, depth of discharge, specific energy and energy density have been evaluated taking as reference the maximum energy to be delivered or stored. Mass and volume of every storage have been evaluated multiplying values of the corresponding cell, for the number of cells. Then, it was further increased of 20%, including balance of plant (BOP).

Table 4. Characteristics of the battery packs

	LFP cells based	**NMC cells based**
Nominal energy (kWh)	83.2	44.4
Maximum current[1] (A)	480	563
Depth of discharge[2] (%)	1%	1%
Mass (kg)	1075	346
Volume (L)	730	173
Specific energy[2] (Wh/kg)	77	128
Energy density[2] (Wh/L)	114	128
Specific power[1] (W/kg)	233	723

1. under maximum solicitation in terms of power
2. under maximum solicitation in terms of energy

As visible, the critical sizing condition for the battery pack based on LFP cell was due the maximum allowed current, equivalent to the maximum limit imposed by the manufacturer (i.e. 480 A), for the corresponding cell. Then, after satisfying the maximum required power, the other two criteria are automatically satisfied. On the other hand, storage system having NMC cells is not exploited at its maximum performance in terms of power, but it requires to be oversized to maintain a reduced depth of discharge (i.e. 1%), thus allowing the hypothesis to cover the whole life of the application. Difference in terms of mass and volume are significantly in favour of the storage system based on NMC cells. However, these aspects are not so critical, being for one stationary application. Then, specific energy and power, and energy density are lower than indicated for the corresponding cells, also due the presence of the balance of plant.

4.2.2. Systems based on supercapacitors

The other examined case refers to the installation of one storage system based on supercapacitors. In fact, since the most frequent working operations are limited in the range 5-15 s, the required energy to be stored is necessarily limited. Indeed, solutions based on supercapacitors may appear as competitive. Further details about performance offered by supercapacitors in comparison with high power lithium batteries are shown in [28]. Also in this case, the considered cell was taken from available products on the market. Main characteristics are shown in Table 5.

Table 5. Characteristics of the SC cell

	Maxwell K2-BCAP3000
Capacitance (F)	3000
Voltage max/nom (V)	2.85/2.7
Nominal energy (Wh)	2.5
Max discharging current peak (A)	1900
Mass (kg)	0.5
Volume (L)	0.4
Specific energy (Wh/kg)	5.1
Energy density (Wh/L)	6.3
Specific power (W/kg)	10800

Also in this case the supercapacitors stack has been sized according the two main power/energy stress conditions already described, i.e. power peaks of 250 kW and 150 kW for 15 s. Requirements in terms of power and energy to be delivered or stored have been widely checked, taking into account the maximum allowed current limits. Following formulas have been used:

$$V_m = n_s \frac{V_{max} + V_{min}}{2} \quad (5)$$

$$E_n = \int v(t)i(t)dt = \frac{1}{2}C\left(V_{max}^2 - V_{min}^2\right) \quad (6)$$

$$P_n = v(t)i(t) = (V_m - R_i I_n)I_n \quad (7)$$

Where V_{max} and V_{min} are respectively the maximum and minimum SC cell voltage, V_m the average stack voltage, n_s the number of cells in series, E_n and P_n are the nominal energy and power respectively, C and R_i are the nominal capacitance and the internal resistance of the SC stack, I_n the nominal current.

As for the previous case, number of SC cells in series has been determined having as constraint the DC bus voltage (5). Then, from energy (6) and power requirements (7), number of elements in parallel can be adapted by opportunely choosing the SC cell.

About stack life, manufacturer guarantees for the supercapacitor cell about 10^6 cycles, considering full depth of discharging. Indeed, depth of discharge must not be limited, as for the sizing of battery pack. As for the battery solution, mass and volume have been evaluated considering balance of plant, by increment of 20%. Table 6 shows the sizing of the SC stack.

Table 6. Characteristics of the SC stack

	SC stack
Nominal energy (kWh)	0.7
Maximum current[1] (A)	476
Depth of discharge[2] (%)	95%
Mass (kg)	156
Volume (L)	125
Specific energy[2] (Wh/kg)	4.2
Energy density[2] (Wh/L)	5.3
Specific power[1] (W/kg)	1686

1. under maximum solicitation in terms of power
2. under maximum solicitation in terms of energy

As observable, the critical sizing condition for the SC stack is due the requirement in terms of energy. In fact, under the solicitation of 150 kW, about 95% of depth of discharge was reached. On the other hand, under solicitation of 250 kW, the maximum current remains significantly far from the maximum limit declared by the manufacturer. Mass and volume are favourable in comparison to the battery pack solutions.

5. Cost analysis

After sizing components and evaluating fuel consumptions of the conventional and hybrid variants, a brief industrial cost analysis divided in capital and running costs has been carried out for some configurations. The analysis was aimed to verify the competitiveness of the hybrid versions respect to the conventional one. Two possible scenarios were considered: in the first one, the standard ICE is maintained unaltered (i.e. the version having 414 kW), and the RESS added to allow the energy recovery. This case represents a soft evolution of the standard RTG, which apart the storage system is maintained unchanged. In the second one, ICE is replaced with one of the gen-sets shown in Table 2. Indeed, the RTG powertrain has evolved significantly. The reduction cost due ICE downsizing and extra-costs due storage systems have been considered (capital part), including reduction in terms of running costs due fuel saving. The following criteria have been used:

- An ICE cost of 100 €/kW was assumed for both the engine used in conventional and hybrid versions.

- A RESS cost of 400 €/kWh and 800 €/kWh was assumed for the LFP and NMC solutions respectively. This cost was then increased by 10%, to consider the assembly of battery pack and the battery management system (BMS).
- A RESS cost of 0.02 €/F was assumed for supercapacitors, additionally increased by 10% to consider the assembly of the supercapacitor stack.
- As far as the electric drive EG, its components price, commercially available, has been evaluated in 100 €/kW for the machine and 50 €/kW for the converter.
- In terms of running cost, a standard scenario in which the RTG crane stays in service for 300 days per year, for a total duration of 10 years, can be assumed.
- Fuel consumption was obtained from experimental campaign, and an average value of 87 L/day has been taken as reference. Starting from that, an extrapolation on year basis has been conducted. On the other hand, fuel consumption for HEV versions was obtained from simulations. Finally, Diesel fuel costs was assumed considering low tax prices for industrial applications, i.e. 1 €/L.
- Maintenance costs have been considered of 1 k€/y for the standard ICE (414 kW), specifically developed for heavy duty applications, reduced to 0.5 k€/y for the downsized ones, of automotive derivation. Substitution of the ICE was not taken into account for the considered useful life. About the RESS, substitution is not required at the same, since the corresponding cycle life overcomes the number of charging-discharging cycles effectively executed during the useful life of the considered application.

Cost analysis for the two scenarios were examined in Table 7. *Standard* is the RTG equipped with the standard ICE (414 kW); *HEV STD* is related to the first examined scenario, i.e. the hybrid architecture equipped with the standard ICE and the energy storage system. *HEV A* is the hybrid architecture equipped with ICE version downsized at 165 kW, while *HEV B* has been downsized until to 36 kW. For *HEV STD*, *HEV A* and *HEV B*, storage based with NMC lithium cells or supercapacitors have been considered. As visible, modification in ICE sizing does not have impact on the RESS sizing, since its sizing condition has been identified for descending operations, when the ICE does not furnish any contribution.

Table 7. Cost analysis

	Standard	*HEV STD Li-bat*	*HEV STD SC stack*	*HEV A Li-bat*	*HEV B Li-bat*	*HEV A SC stack*	*HEV B SC stack*
Parts							
ICE (k€)	41.4	41.4	41.4	16.5	3.6	16.5	3.6
EG (k€)	62.1	62.1	62.1	24.8	5.4	24.8	5.4
RESS (k€)	-	39.0	17.0	39.0	39.0	17.0	17.0
Total (k€)	103.5	142.5	120.5	80.3	48.0	58.3	26.0
Usage costs							
Fuel (k€/y)	26.1	18.3	18.3	10.5	10.5	10.5	10.5
Maintenance (k€/y)	1.0	1.0	1.0	0.5	0.5	0.5	0.5
Total (k€/y)	27.1	19.3	19.3	11.0	11.0	11.0	11.0

As noticeable, the first scenario implies an initial extra-cost given by the addition of the storage system. Considering usage costs per year (see Figure 7) respect to the *Standard* version, (i.e. from 27.1 k€/y up to 19.3 k€/y) payback time is within 6 years for the *HEV STD* equipped with lithium battery, and within 3 years with the supercapacitor stack.

If the second scenario is considered, conversely to what happens in other hybrid propulsion system applications [21] [22], cost analysis already supports hybridisation in capital costs. In fact, cost-saving due the downsized ICE covers the extra-cost for the RESS in all the considered cases, guaranteeing a cost benefit from about 24 k€ up to 78 k€. Additionally, usage costs are significantly reduced, from 27.1 k€/y up to 11 k€/y.

It is also evident the convenience of the RESS based on supercapacitors, around one half in terms of cost respect to the lithium battery solution. Regarding lithium batteries, despite the high difference in terms of cell cost (400 €/kWh for LFP vs 800 €/kWh for NMC), it must be stated that final cost for the LFP solution would be substantially aligned (37 k€) with the other one. However, lithium batteries allow much more flexibility since the significantly higher amount of energy stored. In this regard, the extra-cost should allow extra-services, i.e. some working phases to be performed in pure electric mode, maintaining the internal combustion engine switched-off.

Conclusions

In conclusion, the hybridization of different rubber tired gantry (RTG) cranes was addressed through a systematic approach, starting from measurements on the existing system, identification of the powertrain architecture, energy management strategy and sizing of components, through the definition of a numerical simulation model.

Different storage systems technologies have been widely investigated. Because of the load profiles clearly oriented towards charging or discharging in a few seconds at high current rates, supercapacitors or high power lithium batteries have to be considered. The comparison between the two technologies has shown how supercapacitors represent the first choice in terms of offered performance and costs, but high power lithium batteries, correctly sized for the application (i.e. limiting depth of discharging to cover the entire application life) may be competitive as well.

The results have shown the general feasibility of hybridization, producing fuel savings of 30% up to 60%, depending on the ICE adopted. Regarding cost analysis, retrofitting operation on the existing machine through the exclusive installation of the storage system is recovered within the useful life. On the other hand, in case of new machine design the extra-costs due storage installations are clearly compensated by the cost saving due usage of a smaller ICE, having further advantages from fuel costs reduction.

References

[1] R. Kuilboer, “Revolutionary new drive design for Rubber Tired Gantry's”, Maxwell: Periodiek der Electrotechnische Vereeniging, 9 (1) (2006) 12-14.

[2] S. Mulder, “Energy Management Strategy for a Hybrid Container Crane”, Master of Science Thesis in Systems and Control at Delft University of Technology. 16 July 2009.

[3] S. Mulder, “Hybrid Container Cranes: An Energy Management Strategy”, Maxwell: Periodiek der Electrotechnische Vereeniging, 13 (1) (2009) 18-21.

[4] H. Hellendoorn, S. Mulder, B. De Schutter, “Hybrid Control of Container Cranes”, IFAC Proceedings volumes 44(1) (2011) 9697-9702, Proceedings of the 18th IFAC World Congress, Milano (Italy), August 28 - September 2, 2011. DOI: 10.3182/20110828-6-IT-1002.00010.

[5] C.E., Knight, V.M. Becerra, W. Holderbaum, R. Mayer, “A Consumption And Emissions Model Of An RTG Crane Diesel Generator”, Proceedings of TSBE EngD Conference, 5 July 2011.

[6] C.E. Knight, V.M. Becerra, W. Holderbaum, R. Mayer, “Modelling and simulating the operation of RTG container cranes”, Proceedings of the 6th IET International Conference on Power Electronics, Machines and Drives (PEMD 2012), 27-29 March 2012. DOI: 10.1049/cp.2012.0362.

[7] M.M. Flynn, P. McMullen, O. Solis, “High-Speed Flywheel and Motor Drive Operation for Energy Recovery in a Mobile Gantry Crane”, Proceedings of the Applied Power Electronics Conference, APEC 2007 - Twenty Second Annual IEEE. 25 Feb.-1 March 2007. DOI:10.1109/APEX.2007.357660.

[8] M.M. Flynn, P. McMullen, O. Solis, “Saving energy using flywheels”, IEEE Industry Applications Magazine, 14(6) (2008) 69-76. DOI:10.1109/MIAS.2008.929351.

[9] W. Liu, Z. Zhu, C. Chang, R. Wang, H. Xu, “Research of System of Energy Recycling on Rubber-Tyred Gantry Crane”, Proceedings of the International Conference on Electrical Machines and Systems, 2008. ICEMS 2008. 17-20 Oct. 2008. 2183-2187.

[10] C. Chang, J. Yang, Z. Zhu, “Research of Supercapacitor Voltage Equalization Strategy on Rubber-Tyred Gantry Crane Energy Saving System”, Energy and Power Engineering, 2(1) (2010) pages 25-30. DOI: 10.4236/epe.2010.21005.

[11] C. Chang, J. Yang, P. Cao, Q. Niu, Z. Zhu, “Study on Supercapacitor Energy Saving System for Rubber-Tyred Gantry Crane”, Proceedings of Power and Energy Engineering Conference (APPEEC), 2010 Asia-Pacific, 28-31 March 2010. DOI:10.1109/APPEEC.2010.5448850.

[12] M. Acciaro, G. Wilmsmeier, “Energy efficiency in maritime logistics chains”, Research in Transportation Business & Management 17 (2015), pages 1–7. DOI:10.1016/j.rtbm.2015.11.002.

[13] Y.C. Yang, W.M. Chang, "Impacts of electric rubber-tired gantries on green port performance", Research in Transportation Business & Management 8 (2013), pages 67–76. DOI: 10.1016/j.rtbm.2013.04.002.

[14] H. Schøyen, S. Bråthen, "Measuring and improving operational energy efficiency in short sea container shipping", Research in Transportation Business & Management, 17 (2015), pages 26–35. DOI: 10.1016/j.rtbm.2015.10.004.

[15] S. Roh, V.V. Thai, Y.D. Wong, "Towards Sustainable ASEAN Port Development: Challenges and Opportunities for Vietnamese Ports", The Asian Journal of Shipping and Logistics, 32(2) (2016), pages 107-118. DOI: 10.1016/j.ajsl.2016.05.004.

[16] Z. Lui, "Concept Design of Hybrid Crane Vessel Feasibility study of utilizing electric energy storage technology", Master of Science Thesis in Marine Engineering at Delft University of Technology, 19 April 2016.

[17] N. Zhao, N. Schofield, W.Q. Niu, "Energy Storage System for a Port Crane Hybrid Power-train", IEEE Transactions on Transportation Electrification, In Press. (2016). DOI:10.1109/TTE.2016.2562360.

[18] P. Fritzson, "Introduction to Modeling and Simulation of Technical and Physical Systems with Modelica", Wiley-IEEE Press, 2011.

[19] M. Rinchi, L. Pugi, F. Bartolini, L. Gozzi, "Design of control system to prevent forklift capsize", International Journal of Vehicle Systems Modelling and Testing, vol. 5 (1), pages 35-58, 2010. DOI: 10.1504/IJVSMT.2010.033730.

[20] B. Allotta, L. Pugi, A. Ridolfi, R. Costanzi, F. Bartolini, N. Monni, M. Natalini, R. Giusti, "An anti-capsize strategy for industrial vehicles: Preliminary testing on a scaled AGV", 10th IEEE/ASME International Conference on Mechatronic and Embedded Systems and Applications (MESA 2014), 2014. DOI: 10.1109/MESA.2014.6935580.

[21] G. Lutzemberger, G. Pede, G. Sanna, H. Tarun, "Systematic development of series-hybrid bus through modelling", Vehicle Power and Propulsion Conference (VPPC 2010), Lille (France), 2010.

[22] A. Bertini, M. Ceraolo, G. Lutzemberger, "Systematic approach in the hybridization of a hydraulic skid-loader", Automation in Construction, vol. 58, pages 144-154, 2015.

[23] M. Ceraolo, A. di Donato, G. Franceschi, "A General Approach to Energy Optimization of Hybrid Electric Vehicles", IEEE Transaction on Vehicular Technology vol. 57 n. 3 (2008), 1433-1441.

[24] M. Ceraolo, G. Lutzemberger, "Energy optimization of hybrid vehicles. A general suboptimal analysis", AEIT Annual Conference, 14-16 Oct. 2015, Naples.

[25] M. Ceraolo, "A new Modelica electric and hybrid powertrains library", Proceedings of the 11th International Modelica Conference, Versailles, France, 21-23 September 2015.

[26] M. Ceraolo, T. Huria, G. Lutzemberger, "Experimentally-determined models for high-power lithium batteries", SAE 2011 World Congress & Exhibition, SAE Technical Paper, 2011-01-1365, http://dx.doi.org/10.4271/2011-01-1365.

[27] M. Ceraolo, G. Lutzemberger, D. Poli: "Aging evaluation of high power lithium cells subjected to micro-cycles", Journal of Energy Storage, vol. 6, pages 116-124, 2016.

[28] M. Ceraolo, S. Barsali, G. Lutzemberger, M. Marracci: "Comparison of SC and high-power batteries for use in hybrid vehicles", SAE Technical Paper 2009-24-0069, 2009.